J. Appl. Comput. Mech., 8(3) (2022) 891-903
DOI: 10.22055/JACM.2020.32954.2112

ISSN: 2383-4536
jacm.scu.ac.ir

Shahid Chamran University of Ahvaz

Journal of Applied and Computational Mechanics

Research Paper

Analytical Solutions and Analyses of the Displacement Separating Point in Diffusers

Ebrahim Sharifi Teshnizi[1], Fereshte Momeni[2]

[1] Department of Mechanical Engineering, Tafresh University, Tafresh, P.O. Box 39518-79611, Iran, E-mail: sharifi@tafreshu.ac.ir
[2] Department of Mechanical Engineering, Kashan University, Kashan, Iran, E-mail: momenifereshte94@gmail.com

Received Mar 15 2020; Revised May 30 2020; Accepted for publication July 06 2020.
Corresponding author: E. Sharifi Teshnizi (sharifi@tafreshu.ac.ir)

Abstract. The main purpose of this study is to develop an understanding of the turbulent boundary layer calculation to analyze displacement of the separating point in diffusers. An approximate method has been used which is based on an analogy with the rheological power law and is applied in the study of non-linear viscous flows. At first, the method has been validated with the experimental data in the same experimental cases study. An appropriate geometric with and without the Nano-fluids in the straight-wall and curved-wall conical diffusers has been investigated. Its analyses output was compared with the results obtained by a numerical code. Also, the proposed method is more practical and can be used in diffuser design procedures.

Keywords: Turbulent boundary layer, Separating point, approximate method, Straight-wall, Curved-wall Conical diffusers.

1. Introduction

A diffuser is a divergence channel which decelerates the velocity and also recovers the pressure head of the fluid. Today, a significant amount of energy passes through the diffusers each year such as in jet engines, compressors, pumps, turbines, air-conditioning equipment in general. This is necessarily done to decrease the fluid velocity and to increase the static pressure during the passage. Optimal performance in diffusers is associated with a reduction of the total pressure losses in the diffuser. Losses in diffusers are classified into two categories: friction and expansion losses. Frictional losses are due to the diffuser's geometry, on its interior wall surface. Expansion losses are due to changes in pressure gradient and velocity field in the diffusers. Since 1960s, researchers have been investigating the reduction of such losses and improvement of the diffuser's performance as well as the separation point of flow and its displacement. Furthermore, to date, studying diffuser's flow has been a challenge in the field of mechanical engineering because of wide application in energy conversion systems. The literature on diffusers exists in large numbers with analytical, numerical and experimental methods. Reporting the nature of the flow in details has not yet been agreed by the researchers in the field and there is still some controversy. Von Den and Tetervin [1] used the shape factor as a criterion to determine the nature of the flow. They concluded that increase in the value of shape factor led to the consequence of the stronger adverse pressure gradient, indicating the beginning of boundary layer separation. Accordingly, the values of the shape factor for the separation point in the laminar and turbulent flow are about 3.5 and 2.4, respectively. As they reported, the basic output of a diffuser was the pressure-recovery coefficient C_P, which was defined as: $C_P = (P_2(x)-P_1(x=0))/(0.5\rho U_0)$, and its ideal value in term of the area ratio ($C_{P,ideal}=1-(A_2/A_1)^{-2}$) was a basic parameter in the diffuser's design. The nature of the flow in the diffuser changes with the air geometry and inlet flow conditions. Whitman et al. [2] examined the effects of the inlet condition of boundary layer of two-dimensional diffusers with flat walls and found that increasing the thickness of the boundary layer at diffusers' entrances could be reducing the diffusers performance. Moore and Kline [3] and Fox and Kline [4] classified the flow in diffuses into four regimes (1- no appreciable stall, 2- Transitory stall, 3- fully developed stall and 4- jet flow). A typical design would have area ratio=5:1, for which the ideal value is C_P=0.96, almost full recovery. In fact, measurements of C_p for the above area ratio are only as high as 0.86 and can be as low as 0.24. Some experimental studies have been conducted by Rao and Raju [5], Furuya et al. [6], Senoo and Nishi [7], Cochran and kline [8] in order to delay the separation point and increase the diffuser's performance, using various mechanisms and techniques such as vortex generators, splitters, suction at the entrance and short flat vanes, respectively. In recent years and the past decade, researches and publications on diffusers have been appeared to be more experimental and numerical. In addition, in some cases the control of separation or study of the above phenomena has been an important issue. For example, Yongsen and Kobayashi [9] used numerical methods and a k-e turbulence model in a conical diffuser, having a total divergence angle of 8° and 30° with a high Reynolds number. They examined the turbulent flow inside the conical diffuser and described the perforated screen effect in order to increase efficiency. Through numerical simulation, Apsley and Leschziner [10] examined the effect of Reynolds number on separation point in diffusers and showed that increasing Reynolds number reduced the separation boundary layer. Experimental methods can be commonly used to determine a diffuser's pressure drop. Thus, by measuring the total pressure at the inlet and outlet of the diffuser, the pressure drop of the

Published online: August 14 2020

diffuser can be measured. Furthermore, the separation point phenomenon and its location can be investigated by measuring the velocity distribution all along the diffuser inside. In this line of research, Singh and Azad [11] measured the characteristics of the turbulent boundary layer and the position of the separating point in a straight-wall conical diffuser. They reported that a total divergence angle of 8°, an area ratio of 4:1, an inlet diameter of 0.1016m and length of 0.745 m were observed. In so doing, hot-wire and pulse-wire anemometry together were used to obtain the results of the complex flow in the conical diffuser. Turbulent flows such as instantaneous flow reversal in the wall region also were investigated. Additionally, Andre Brunn and Wolfgang N. [12] investigated separation control in turbulent flow through an axisymmetric diffuser. They aimed to examine the separated flow effect in diffusers in order to reduce the separation length for the aim of minimizing the related pressure losses. For this aim, the measurements were conducted in a closed pipe-flow channel with an optically fully accessible test section via a laser Doppler velocimeter. In an experimental investigation, Charry et al., [13] studied the separated flow in a three-dimensional diffuser. Furthermore, Johan Ohlsson et al. [14], in a numerical simulation (DNS) in the similar cases, provided accurate and detailed information about the flow physics which have been confirmed by the experimental data. Similarly, Dehghani [15] numerically examined the nanofluid inside a plane diffuser with Cu-water with the finite volume method. As he concluded the steady nanofluid flow was assumed incompressible, laminar, and Newtonian. His study considered the influence of Reynolds number in the range of 100 to 500 and volume fraction of nanoparticles (ϕ<0.05) on the skin friction coefficient and pressure recovery coefficient. The essential reason for the discrepancy in C_P was the flow separation. All in all, the increasing pressure in the diffuser is an unfavorable gradient, which can lead to viscous boundary layers to separate from the wall and significantly reduce the performance. Consequently, controlling the separation and maintaining the attached flow at some diffusers can be efficient in development of the diffuser design. Therefore, we analyzed a novel interesting solution in this research, intending to develop the rheological theories which would predict this behavior more realistically. Askovic R., [16] has developed a new variant of the phenomenology semi-empiric turbulent boundary layer theory that is founded on analogy with the rheological power laws widely used in the study of non-linear viscous flows. It is also to be noted that this phenomenologic theory has been applied and confirmed by Askovic R. [17] in some cases of turbulent boundary layer. Estimation of pressure drop and separation point are the great importance for diffuser design procedure. In this paper, in order to improve the diffusers performance by prescribing a velocity distribution in diffusers, the separation point was practically predicted and its location could be shifted by choosing appropriate geometry. In the first part of this paper, an approximate method in base of the rheological power laws has been proposed to explain turbulent boundary layers in the conical subsonic diffusers. In the second part, the problem is detailed in a subsonic straight-wall conical diffuser and validate with the experimental studies and, in the third part, the method developed in curved-wall conical diffuser in order to reduce the separation length and thus to minimize the related pressure losses; and then the separation point with and without nanofluid, numerically has been investigated.

2. Basic Equations

The flows near a surface where viscous forces are important are known as the axisymmetrical turbulent boundary layer equations which for two-dimensional incompressible flow are written as:

$$\begin{aligned} &\bar{u}\frac{\partial \bar{u}}{\partial x}+\bar{v}\frac{\partial \bar{u}}{\partial y}=u_e u_e'+\frac{1}{\rho}\frac{\partial \tau_t}{\partial y},\\ &\frac{\partial (r\bar{u})}{\partial x}+\frac{\partial (r\bar{u})}{\partial y}=0, \end{aligned} \tag{1}$$

where (x, y) are orthogonal curvilinear coordinates and $(\bar{u}, \bar{v})$ are velocity components at (x, y) in the boundary layer while the external velocity is represented by $u_e(x)$. Both viscosity and turbulence contribute to the shear stress global as follows:

$$\tau_t=\mu\frac{\partial \bar{u}}{\partial y}-\rho\overline{u'v'}=\mu\frac{\partial \bar{u}}{\partial y}+\tau \tag{2}$$

Due to the rheological power low, the *Prandtl turbulence model* has been used:

$$\frac{1}{\rho}\tau=\nu k_n T^n\frac{\partial \bar{u}}{\partial y}, \tag{3}$$

$$T=\frac{y^2}{\nu}\left|\frac{\partial \bar{u}}{\partial y}\right|. \tag{4}$$

with the boundary conditions:

$$\left.\begin{aligned} &\bar{u}=\bar{v}=0,\ \frac{\partial \bar{u}}{\partial y}\to\infty \quad \text{for} \quad y=0,\\ &\bar{u}=u_e(x),\ \tau=0 \quad \text{for} \quad y=\delta(x) \end{aligned}\right\} \tag{5}$$

and initial condition:

$$\bar{u}=u_0(y),\quad \text{for}\quad x=x_0, \tag{6}$$

where $\delta(x)$ is the boundary layer thickness. After integrating the system equations (1), the *momentum equation* results in the following form:

$$\frac{d\delta_2}{dx}+\frac{u_e'\delta_2}{u_e}(2+H)=\frac{1}{2}c_f. \tag{7}$$

If $\bar{v}$ is eliminated from the system of equations (1):

$$\bar{v} = -\int_0^y \frac{\partial \bar{u}}{\partial x} dy - \frac{r'}{r}\int_0^y \bar{u} dy$$

it gives:

$$\frac{1}{\rho}\frac{\partial \tau_t}{\partial y} = -u_e u_e' + \bar{u}\frac{\partial \bar{u}}{\partial x} - \frac{\partial \bar{u}}{\partial y}\int_0^y \frac{\partial \bar{u}}{\partial x} dy. \tag{8}$$

3. Falkner-Skan Equation

By substituting τ, T, u_e, and $\bar{u}$, into equation (8), and after carrying out several transformations, it follows:

$$\begin{aligned} &k_n (\bar{x} - \bar{x}_0)^{\alpha(1+n)-3\beta} \cdot \left(t^n F''\right)' = \\ &(\bar{x} - \bar{x}_0)^{2(\alpha-\beta)-1}\left[(\alpha-\beta)F'^2 - \alpha F F''\right] - m(\bar{x} - \bar{x}_0)^{2m-1}. \end{aligned} \tag{9}$$

The differential equation (9) was recently numerically resolved by Askovic [16] for various pairs of values n and k_n. The values of $n = 0.66$ and $k_n = 0.55$ have the greatest significance for the calculation of the axisymmetrical turbulent boundary layers.

3.1. Approximate method to calculate the axisyimmetrical turbulent boundary layer for arbitrary $u_e(x)$

Introducing at first:

$$\begin{aligned} g(x) &= \frac{\nu}{u_e^2} u_e'. \\ u_e(x) &= C|x - x_0|^m = U_0 |\tilde{x} - \tilde{x}_0|^m \end{aligned} \tag{10}$$

with $\tilde{x}_0 = U_0 . x_0 / \nu$ and applying (10), it is found that:

$$g(x) = m(\bar{x} - \bar{x}_0)^{-(1+m)}.$$

Moreover, by introducing the following non- dimensional quantity;

$$Q(x) = g\left(R^{**}\right)^{2-n},$$

where we have

$$R^* = \eta^* \left(\frac{m}{g}\right)^{\frac{1}{2-n}}, \quad R^{**} = \eta^{**}\left(\frac{m}{g}\right)^{\frac{1}{2-n}}, \; C_f = 2c\left(\frac{m}{g}\right)^{\frac{1-n}{2-n}},$$

It could be found that

$$c_f (R^{**})^{1-n} = 2C\left(\frac{m}{g}\right)^{\frac{1-n}{2-n}}\left[\eta^{**}\left(\frac{m}{g}\right)^{\frac{1-n}{2-n}}\right] = 2C(\eta^{**})^{1-n} = G(Q) \tag{11}$$

where $H = \delta_1 / \delta_2 = \eta^{**} / \eta^* = H(Q)$. Equation (11) may be accepted as approximately valid in a more general case for which $u_e(x)$ is an arbitrary function. The parameter Q(x) can be determined by replacing expressions (11) into (7), which is transformed into the form:

$$\frac{1}{2-n}\frac{d}{dx}\left(R^{**}\right)^{2-n} + (1+H)\frac{u_e g}{\upsilon}\left(R^{**}\right)^{2-n} = \frac{1}{2}\frac{u_e c_f}{\upsilon}\left(R^{**}\right)^{1-n}. \tag{12}$$

Thus, a differential equation results for calculating Q(x) as:

$$\frac{dQ}{dx} + E(Q)\frac{u_e'}{u_e} = \frac{u_e''}{u_e} Q, \tag{13}$$

where

$$E(Q) = (2-n)\left[(1 + H(Q))Q - \frac{1}{2}G(Q)\right] + 2Q. \tag{14}$$

The best agreement was obtained with the experimental results in the case in which n=0.66 and $k_n = 0.55$ were taken to determine $E(Q)$. In this particular case, detailed computations have been carried out regarding the functions $G(Q)$, $E(Q)$ and $H(Q)$ by the series expressions:

$$E(Q) = -0.063 + 4.097Q - 23.163Q^2,$$
$$G(Q) = +0.0938 + 2.1143Q + 36.1035Q^2 + 984.7348Q^3, \quad (15)$$
$$H(Q) = 1.6529 - 2.17Q.$$

Thus, by inserting equation (15) into (13), for an approximate calculation of the turbulent boundary layer, in the case of n=0.66, we obtained a Riccati like differential equation:

$$\frac{dQ}{dx} + (-0.063 + 4.097Q - 23.163Q^2)\frac{u_e'}{u_e} = \frac{u_e''}{u_e'}Q. \quad (16)$$

In order to avoid the singularity due to the function u_e' in zero, equation (16) should be changed in the following way:

$$Z = \frac{Q}{g} = \left(R^{**}\right)^{\frac{4}{3}} = \left(\frac{u_e\delta_2}{\nu}\right)^{\frac{4}{3}}. \quad (17)$$

with the new function $z(x)$, equation (16) reduces to a Riccati like equation:

$$\frac{dz}{dx} - 23.163\frac{\upsilon}{u_e^3}(u_e')^2z^2 + 2.097\frac{u_e'}{u_e}z = 0.063\frac{u_e}{\nu}. \quad (18)$$

The approximate method in order to calculate the turbulent boundary layer proposed in this study consists of the following steps:

- At first, for a given $u_e(x)$, the differential equation (18) is to be integrated with a prescribed initial condition of δ_2:

$$z = \left(\frac{u_e\delta_2}{\nu}\right)^{\frac{4}{3}} = z_1 \quad \text{for} \quad x = x_1 \quad (19)$$

- After finding $z(x)$, δ_2 has been determined by using equation (19), $Q(x)$ has been given by equations (10) and (17): $Q(x) = g(x)z(x)$.
- The next step is to determine the function $G(Q)$ and $H(Q)$ by using the relationship (15).
- The formulas:

$$H(x) = H(Q), \quad C_f = z^{-1/4}G(Q), \quad (20)$$

- Offering two characteristics of the turbulent boundary layer. In order to demonstrate and validate the approximate method developed above, the interesting case in the straight and curved-wall conical diffusers was chosen and stated in the following sections.

4. Turbulent Boundary Layer in the Straight-wall Conical Diffusers

To apply the approximate method in this case, a flow produced by a punctual source and limited by conical divergent walls is supposed. The geometrical parameters are shown in figure 1, where R_1 and θ are respectively the diffuser inlet radius and half angle.

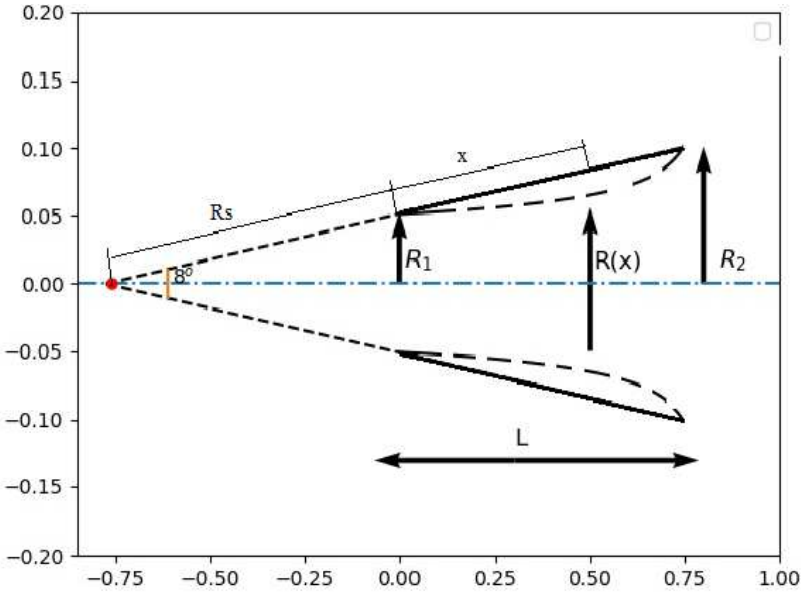

Fig. 1. Geometry of the straight-wall conical diffuser.

The distribution of the external velocity $u_e(x_n)$ for it is given by:

$$u_e(x) = \frac{U_0 R_S^2}{(R_S + x)^2}, \tag{21}$$

$$R(x) = (R_S + x)\sin\theta, \tag{22}$$

where $U_0 = u_e(x = 0)$ and $R_1 = R_S \sin\theta$. Let the velocity $u_e(x)$ at the external frontier of the boundary layer be given by:

$$u_e(x) = C(R_S + x)^m, \tag{23}$$

where $C = U_0\ R_S^2$ and m =-2. If we replace (21) and (22) into (16), then it results:

$$(R_S + x)\frac{dQ}{dx} = 23.163\ m\ Q^2 - (\frac{7}{3} + 3.097\ m)Q + 0.063\ m\ , \tag{24}$$

Introducing the new variable: $\lambda = 23.163\ m\ \ln(R_S + x)$, equation (24) reduces to:

$$\frac{dQ}{d\lambda} = Q^2 - (0.1337 + \frac{0.10073}{m})\ Q + 0.00272. \tag{25}$$

It is easy to show that the solution of equation:

$$Q^2 - (0.1337 + \frac{0.10073}{m})\ Q + 0.00272 = 0 \tag{26}$$

are imaginary if:

$$-3.42847 < m < -0.42418, \tag{27}$$

where the real ones for all the other values of m are out of the interval. The general solution is as the following:

$$\frac{1}{p}\text{arctg}\frac{1}{p}(Q - \frac{0.050365}{m} - 0.06685) = \lambda + \lambda_0, \tag{28}$$

i.e., choosing the integration constant in the form: $\lambda_0 = -23.163m.\ln C_0$, when the new function, offering the parameter $Q(x)$ is defined by:

$$Q(x) = 0.06685 + \frac{0.050365}{m} + p\ \text{tg}\left[23.163mp\ \ln(\frac{R_S + x}{C_0})\right] \tag{29}$$

where

$$p = \sqrt{-0.001747 - \frac{0.006732}{m} - \frac{0.002537}{m^2}}. \tag{30}$$

The general solution is in the following form:

$$Q(x) = 0.04167 - 0.03138\ \text{tg}\left[1.45371\ \ln(\frac{R_S + x}{C_0})\right], \tag{31}$$

where P=*0.03138* and $C_0 = 0.52916R_S$. The new function, offering the parameter $Q(x)$, is defined by:

$$Q(x) = 0.04167 - 0.03138\ \text{tg}\left[1.45371\ \ln(1+\frac{x}{R_S}) + 0.92523\right] \tag{32}$$

after substituting equation (17), we have:

$$z(x) = \left(0.01569\ \text{tg}\left[1.45371\ \ln(1+\frac{x}{R_S}) + 0.92523\right] - 0.02083\right)\frac{R_e}{(1+\frac{x}{R_S})}. \tag{33}$$

By determining the function $z(x)$ and $Q(x)$, all the characteristics of the global boundary layer as well the momentum thickness can be calculated as:

$$\frac{\delta_2}{R_S} = \frac{1}{R_e}(1+\frac{x}{R_S})^2 z^{3/4}. \tag{34}$$

5. Validation

In order to validate the approximate method in conical diffusers, the experimental study of Singh and Azad [11] is preferred. In this study, the characteristics of the turbulent boundary layer and the position of the separating point in a conical diffuser have been investigated. The conical diffuser had a total divergence angle of 8°, inlet diameter of *0.1016m* with a length of *0.745m*. The

obtained results can be used as a test case for the development, verification, and realization of engineering calculation methods to predict flow in conical diffusers. Some of the experimental results of these authors have been compared with the present results obtained by the approximate method. In particular, the details of the results correspond to the separating point. The approximate method has been applied to the same geometry with a flow condition as used by these authors which is presented in the following.

For all the measurements, the Reynolds number of flow has maintained based on the initial velocity and inlet diameter Di (the inlet section of the diffuser). In the experimental study, it has been reported that the recirculation flow starts at position 2, X=0.156 *m* at the wall, which increases as the flow moves towards the diffuser exit. This position corresponds to the position of the initial separation.

Table 1. Characteristics of the turbulent boundary layer in the straight-wall conical diffuser.

x(m)	Q(x)	G(Q)	z(x)	$\delta 2$ (m)	H(x)	$C_f(x)$
0.030	-0.0055	0.0830	1075.89	0.00336	1.665	0.015
0.060	-0.0120	0.0720	2218.24	0.00368	1.679	0.011
0.090	-0.0190	0.0600	3463.10	0.00402	1.695	0.007
0.120	-0.0280	0.0410	4858.60	0.00441	1.714	0.004
0.155	-0.0410	0.0016	6769.26	0.00497	1.741	0.001
0.160	**-0.0430**	**- 0.0072**	**7075.28**	**0.00506**	**1.746**	**0.000**

6. Comparison of Approximate Method with the Experimental Data

The most important characteristics of the turbulent boundary layer of a conical diffuser calculated by the approximate method have been compared with the same geometry and similar flow condition which was used by Singh and Azad [11]. The divergence angles $2\theta = 8^{\circ}$, inlet section, R_1 = 0.0508 *m*, input debit flow, $\dot{V} = 85.08$ *l/s* the kinematic viscosity of fluid, $\nu = 1.54 \cdot 10^{-5}\, m^2/s$, and the Reynolds number $Ret = U_0 D_0/\nu$ was maintained 6.9×10^4 based on U_0 and the inlet diameter of the diffuser.

It can be seen that the separating point of the boundary layer (*G*(*Q*)=0 appears at *X*=0.15 *m*. This value corresponds to station 2 in the experimental data of Singh et al. [11] where the parameter γ_p is about 0.99 and matches the position of the initial separation point. This gives a deviation of about 10% from the abscise of the separation point related to the instantaneous recirculation that begins at about the wall and increases when the flow moves towards the output of the diffuser (see Figures 2 and 5).

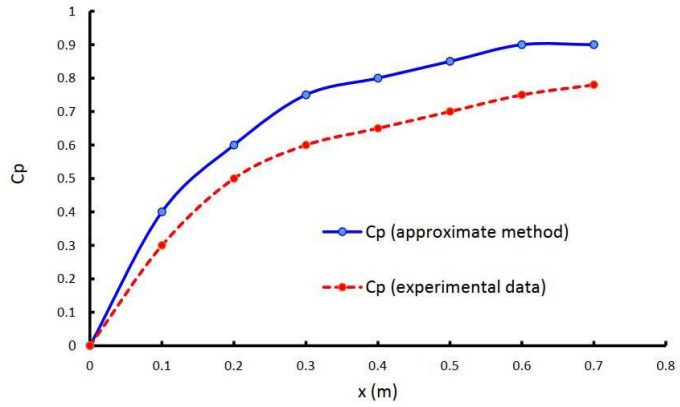

Fig. 2. Comparison of C_P with approximate method and the experimental data.

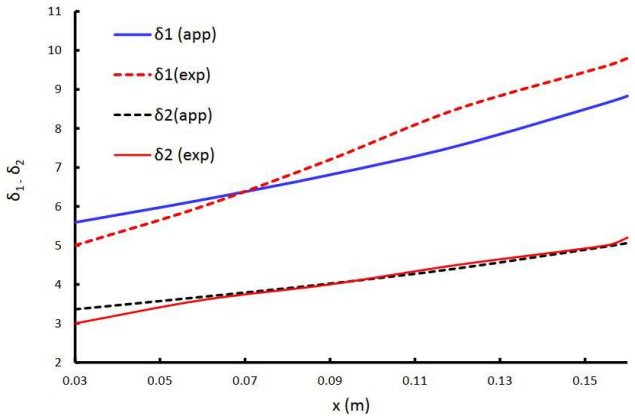

Fig. 3. Comparison of δ_1 and δ_2 obtained by the approximate method and the experimental data.

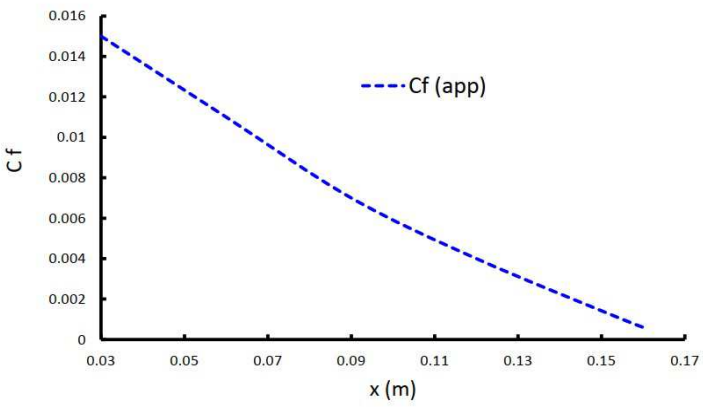

Fig. 4. Distributions of the friction coefficient (C_f) along the longitudinal direction obtained by the approximate method.

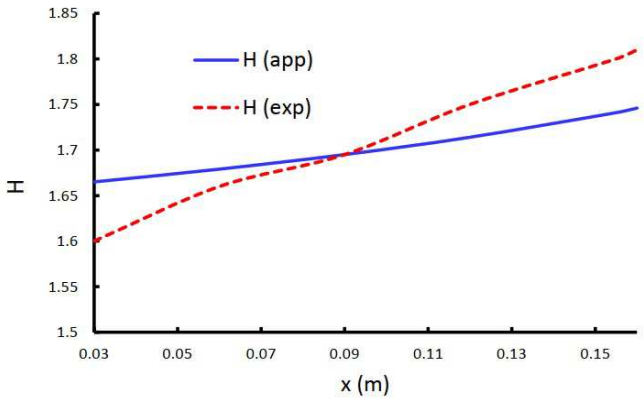

Fig. 5. Comparison of *H* obtained by approximate method and the experimental data.

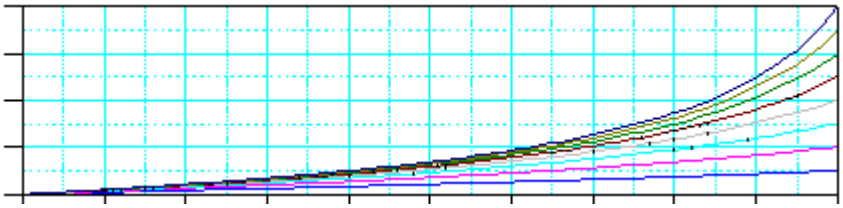

Fig. 6. A family of diffuser of types $(dp/dx = const)$.

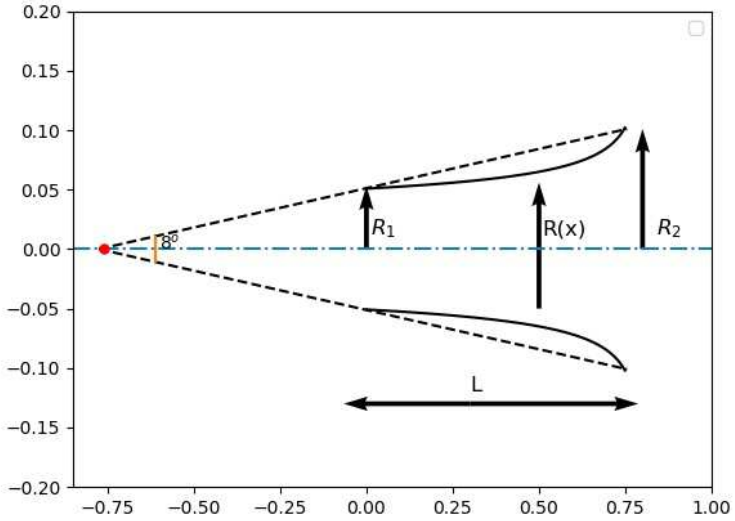

Fig. 7. Geometrical relation of the curved-wall conical diffuser.

By the distribution of the friction coefficient, the separating point could be predicted. The results in the experimental data showed that the friction coefficient significantly decreased about 80% of its initial value at x= 0.2 m at the entrance of the diffuser (Figure 4-7). The separating point of the boundary layer calculated by the approximate method (Cf=0) appeared at x=0.155m. From this point of view, it can also be concluded that the prediction of the separating point with the approximate method was also reasonable. In Figures 2 to 5, the results obtained by the approximate method are compared with the experimental data of Singh and Azad [11].

These results show that there are average deviations of %20, %10, %7, and %5, assigned to C_P , δ_1, δ_2 , and H respectively. Thus, it can be observed that the trend of the curve relative to the approximate method is a good match with the experimental results.

7. Turbulent Boundary Layer in Curved-wall Conical Diffuser

The central problems of diffuser design are prediction and prevention of flow separation. In this case, the calculation method is basically the same as that for the conical diffuser, except that the geometrical relations require the radii for curve diffusers rather than the straight-wall. In these types of diffusers, increasing the opening passage occurs more slowly at the beginning than at the end so that the pressure gradient is more continuous. Thus, the main cause of separation flow and consequently the main source of losses are considerably reduced. From this point of view, the best diffuser is that in which, for potential flow, the pressure gradient remains relatively constant along with the diffuser $(dp/dx = const)$. Accordingly, geometrical relations of curved-wall conical diffusers are expressed as (see Fig. and equation (35)):

$$R(x) = \frac{R_2}{4\sqrt{1-\left[\left(\frac{R_2}{R_1}\right)^2 - 1\right].\left(\frac{x}{L} - 1\right)}}, \qquad 0 \le x < \frac{(\frac{R_2}{R_1})^4.L}{(\frac{R_2}{R_1})^4 - 1}. \tag{35}$$

In figure 6, a family diffusers of obtained by equation (35) are shown. To apply the approximate method in curved-wall conical diffusers, similar to the previous example, flow is produced by a punctual source but in this case, limited by divergent curved-walls. The geometrical parameters are shown in figure 7, where R_1 and θ is the diffuser inlet radius and half-angle respectively.

where $R_1 = R(x=0)$ and $R_2 = R(x=L)$. The distribution of the external velocity $u_e(x)$, for the curved- wall diffuser is given by:

$$u_e(x) = U_0(1 - \frac{d.x}{L})^{\frac{1}{4}}, \qquad 0 \le x < \frac{L}{d} \tag{36}$$

where $U_0 = u_e(x=0)$, $d = 1-(R_1 / R_2)^4$. In the case of the turbulent boundary layer, according to the method developed above, first of all, we should solve the problem in general manner.

$$u_e(x) = C(\frac{L}{d} - x)^m, \tag{37}$$

where $C = U_0(L/d)^{-m}$ and $m = 1/4$. Replacing (37) into (16), to find out that:

$$(\frac{L}{d} - x)\frac{dQ}{dx} = -23.163\ m\ Q^2 + (0.66 + 3.097\ m)Q - 0.063\ m\ . \tag{38}$$

Introducing the new variable:

$$\lambda = 23.163\ m\ \ln(\frac{L}{d} - x)\ , \tag{39}$$

The last equation reduces to:

$$\frac{Q - Q_1}{Q - Q_2} = \left(\frac{\frac{L}{d} - x}{c_0}\right)^{23.163.m.(Q_1 - Q_2)}. \tag{40}$$

Thus, finally:

$$Q(x) = \frac{Q_1 - qQ_2}{1 - q}, \tag{41}$$

using the abbreviation:

$$q(x) = \left(\frac{\frac{L}{d} - x}{c_0}\right)^{23.163.m.(Q_1 - Q_2)}, \tag{42}$$

where the integration constant c_0 will be calculated with the help of the initial condition (17); while according to (10) and (37), we have:

$$g(x) = \frac{-md}{R_e}(1 - \frac{dx}{L})^{-m-1}, \tag{43}$$

i.e., $g(0) \neq 0$, then the condition $z(0) = 0$ involves $Q(0) = 0$, taking into account (41) and (42), it results:

$$c_0 = (\frac{L}{d})(\frac{Q_2}{Q_1})^{\frac{1}{23.163m(Q_1 - Q_2)}}, \tag{44}$$

The solution of equation (38) was determined completely:

$$q(x) = \frac{Q_1}{Q_2}(1 - \frac{d}{L}x)^{23.163m(Q_1 - Q_2)}. \tag{45}$$

The general solution of the differential equation (38), offering parameter Q(x), is defined by:

$$Q(x) = \frac{0.1755 - 0.1755(1 - \frac{d}{L}x)^{1.853}}{1 - 11.28(1 - \frac{d}{L}x)^{1.853}} \tag{46}$$

After determining the functions $z(x)$ *and* $Q(x)$, we can calculate now all global boundary layer characteristics as well as δ_2 by (19) and the other functions G(x), $H(x)$ et $C_f(x)$. In order to study the separation point of turbulent boundary in a straight-wall conical diffuser, considered in 4, and compared with curved-wall conical diffusers, the numerical example in particular case has been computed. The case of curved-wall conical diffuser, in the same condition flow and geometrical corresponding, has been regarded.

8. Numerical Example

- Turbulent boundary layer in the curved-wall conical diffusers.

The distribution of the external velocity $u_e(x_n)$ for it is given by equation (36) and the particular parameter as follows:

$$R_1 = 0.05\ m,\ \ R_2 = 0.4\ m,\ \ L = 0.745\ m \text{ and } 2\theta = 8^\circ \text{ with the initial velocity } U_0 = 10.5\ m/s \text{ and}$$
$$R_{eL} = \frac{U_0.D_i}{\nu} = \frac{13 \cdot 1}{1.52 \cdot 10^{-5}} = 6.9.10^4 \tag{47}$$

For this case study, the results are given in Table 2, where it is clear that the separation point of turbulent boundary layers $Q(x) = -0.041$ appears at x_n=0.55, indicating considerable displacement of separation point. The other characteristic of the turbulent boundary layer, given by table 2 and figures 8, appears to be also physically acceptable.

Table 2. Characteristics of the turbulent boundary layer in the Curved-wall conical diffuser.

$x(m)$	$z(x)$	$Q(x)$	$G(Q)$	δ_2 (m)	$H(Q)$	δ_1 (m)	$C_f(x)$	$C_F(x)$
0.05	2723.88	-0.0013	0.091	0.0004	1.656	0.0007	0.0130	0.038
0.15	8395.35	-0.0044	0.085	0.0011	1.662	0.0018	0.0090	0.113
0.25	14500.0	-0.0087	0.078	0.0017	1.672	0.0029	0.0070	0.188
0.35	21129.0	-0.0150	0.067	0.0024	1.685	0.0040	0.0060	0.263
0.45	29240.0	-0.0240	0.051	0.0032	1.704	0.0055	0.0040	0.338
0.55	**39260.0**	**-0.0380**	**0.011**	**0.0042**	**1.736**	**0.0074**	**0.0008**	**0.413**

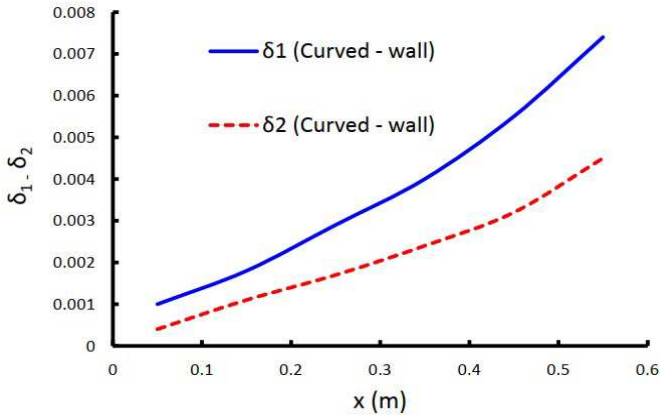

Fig. 8. Evolution of δ_1 and δ_2 in the curved-wall conical diffuser.

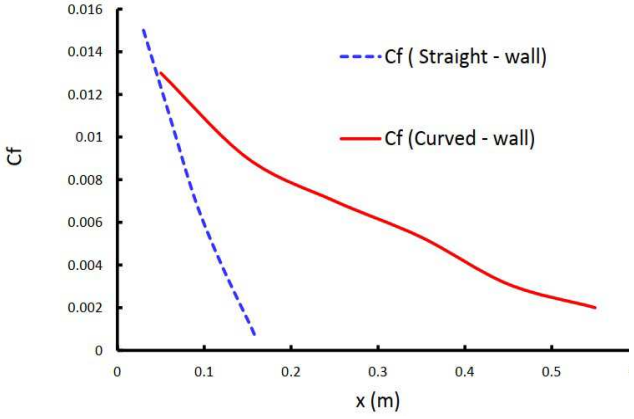

Fig. 9. Distributions of the friction coefficient (C_f) along the longitudinal direction, obtained by the approximate method in straight-wall and curved-wall diffusers.

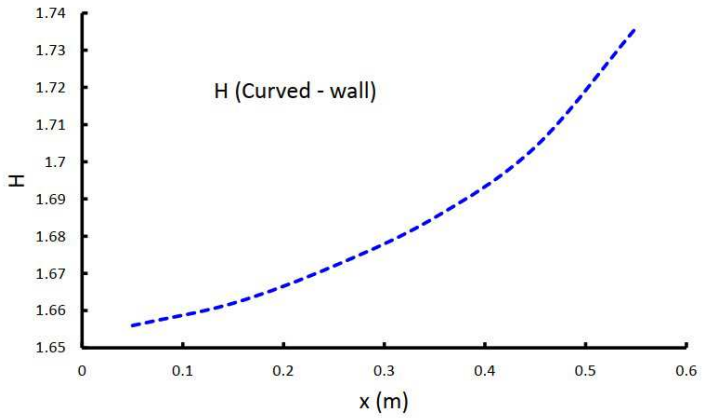

Fig. 10. Evolution of H in the curved-wall conical diffuser.

9. Nanofluid Effectiveness on the Diffuser Performance

As mentioned, control of separation and maintaining the attached flow through the diffusers is a favor in the diffuser design and development to minimize the related pressure losses. In the practical techniques, the aspiration, blowing, vanes deflector, and other features had been used to better control the separation flow. One probability for this proposition can be using nanofluid and, by this, changing the condition flow is meant. In all the fluid properties, viscosity requires the greatest effects in the study of fluid flow. Normally, the viscosity μ is referred to as absolute viscosity in kinematic viscosity relation $(\nu = \mu / \rho)$. Inlet Reynolds number $(R_e=U_0.D_i/\nu)$ is a function of ν, the kinematic viscosity. Therefore, the effect of the nanoparticle addition on the pressure recovery coefficient in Reynold number is investigated in this study. There are some existing formulas to estimate the viscosity of nanofluids. Although extensive research has been carried out in this field and it still needs more attention [18]. Some papers have reported results on the effects of particle shape, particle size, volume fraction, and temperature on nanofluids. Wide variations exist in the development of these studies. Classical models for the description of nanofluid viscosity can be found in the literature such as Einsten Model, Brickman Model, and Batchelor Model. In addition, in these models, the effects of the other factors such as aggregation, dispersion techniques, acidity or PH value, etc. have not been reported. So, in this study, the viscosity of nanofluids has been examined based on rheological study (Krinenger and Dougherty Model) as the following:

$$\mu_{nf} = \mu_{bf}\left(1-\frac{\varphi}{\varphi_m}\right)^{-\eta\varphi_m} \tag{48}$$

where, μ_{nf} is dynamic viscosity of the nanofluid (m. Pa. s) and μ_{bf} is dynamic viscosity of the base fluid. Moreover, φ is volumetric fraction of particle with φ_m = 0.49-0.54 *and* η = 2.5. By choosing a particle-water nanofluid, the mass density can be

calculated by:

$$\rho_{nf} = \varphi.\rho_P + (1-\varphi).\rho_{bf} \tag{49}$$

where: ρ_{nf} nanofluid density, ρ_P particle density and ρ_{bf} based fluid density in (kg/m^3).

10. Numerical Example and Results

Calculation of the turbulent boundary layer in the curved-wall conical diffusers has been investigated using different particle-water nanofluid in the same case using the approximate method. The distribution of the external velocity $u_e(x_n)$ for it is given by equation (36) and the particular parameter as follows: $R_1 = 0.05m$, $R_2 = 0.4m$, $L = 0.745m$, $2\theta = 8^\circ$ and $D_i = 0.1m$.

(R_e=$U_0.D_i/\nu_{nf}$ = $6.9.10^4$) Reynolds number is regarded constant.

φ = 0.05 Cu, φ = 0.95 water volumetric fraction

μ_w = 10^{-3} $N.s/m^2$, ρ_w = 1000 kg/m^3, μ_{nf} = $1.14.10^{-3}$.

Table 3. Characteristic of different particle-water nanofluid.

Nanofluid	ρ_w (kg/m^3)	ρ_{np} (kg/m^3)	ρ_{nf} (kg/m^3)	μ_{nf} (N.s/m^2)	ν_{nf} (m^2/s)	U_0 (m/s)	R_e=$U_0.D_i/\nu$	S. P.
TiO_2- Water	1000	4250	1161	$1.14.10^{-3}$	$2.68.10^{-7}$	0.18	$6.9.10^4$	0.47
Al_2O_3- Water	1000	3900	1145	$1.14.10^{-3}$	$9.96.10^{-7}$	0.67	$6.9.10^4$	0.48
CuO- Water	1000	3620	**1131**	$1.14.10^{-3}$	$1.00.10^{-6}$	0.69	$6.9.10^4$	0.45
Cu- Water	1000	8933	8933	$1.14.10^{-3}$	$8.16.10^{-7}$	0.56	$6.9.10^4$	0.48

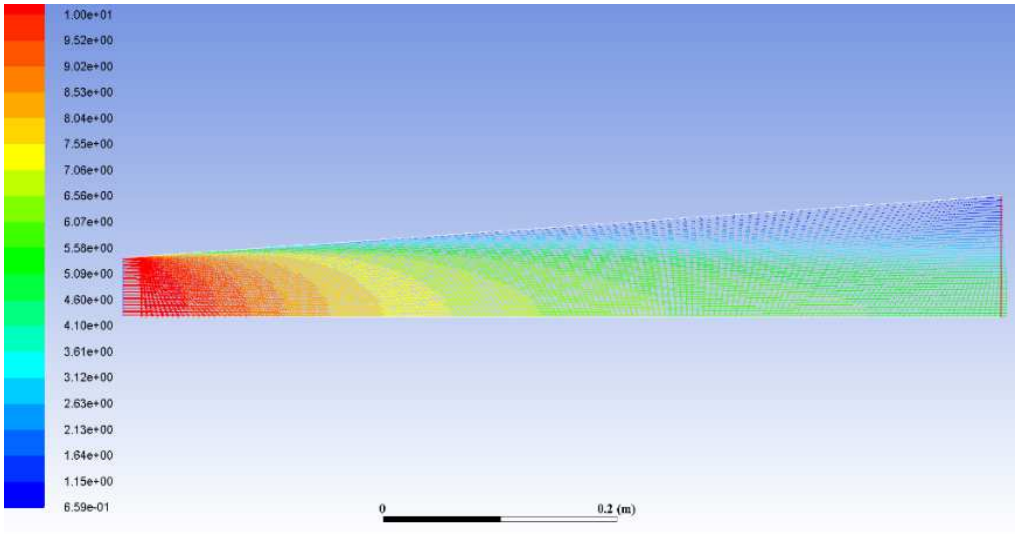

Fig. 11. Distributions of the velocity obtained by numerical method in straight-wall diffusers.

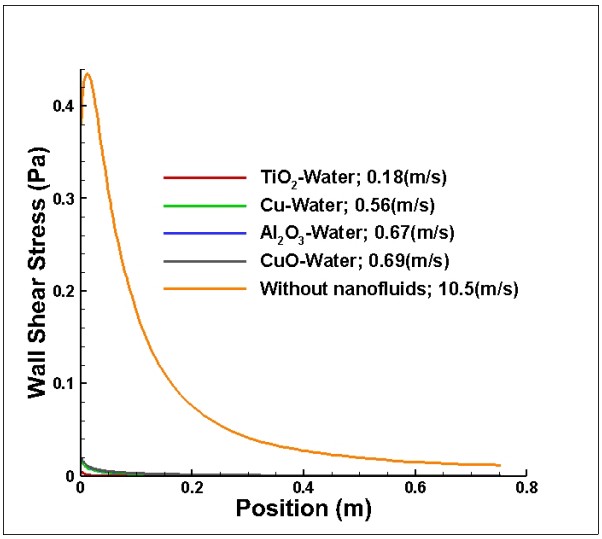

Fig. 12. Distributions of the Wall Shear Stress along the longitudinal direction, obtained by numerical method in straight-wall diffusers with and without the nanofluids.

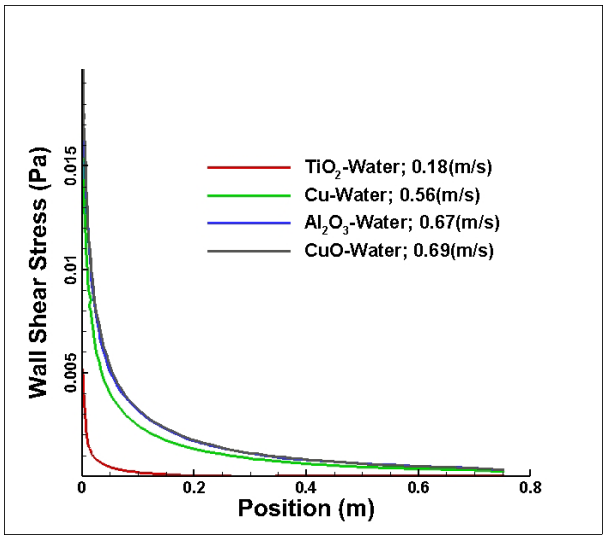

Fig. 13. Distributions of the Wall Shear Stress along the longitudinal direction, obtained by numerical method in straight-wall diffusers with the nanofluids.

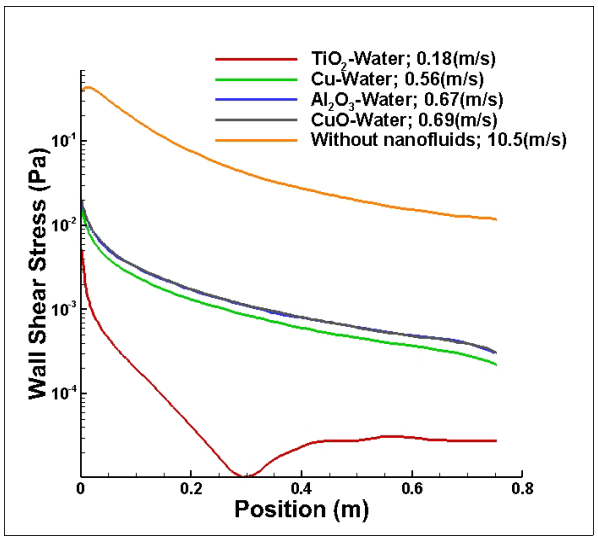

Fig. 14. Distributions of the Wall Shear Stress along the longitudinal direction, obtained by numerical method in straight-wall diffusers with the nanofluids (in logarithmic scale).

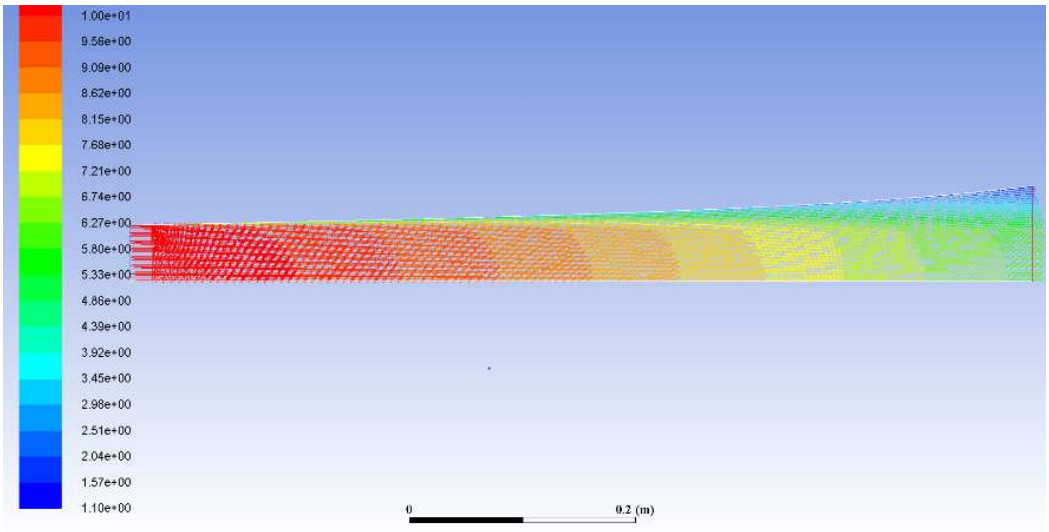

Fig. 15. Distributions of the velocity obtained by numerical method in curved-wall diffusers

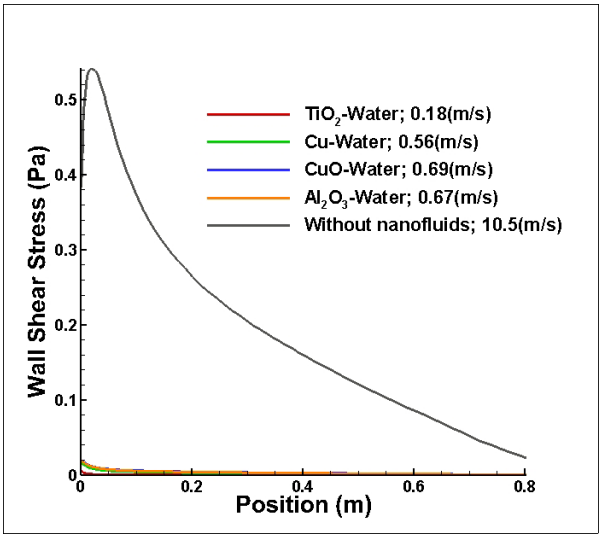

Fig. 16. Distributions of the Wall Shear Stress along the longitudinal direction, obtained by numerical method in curved-wall diffusers with and without nanofluids.

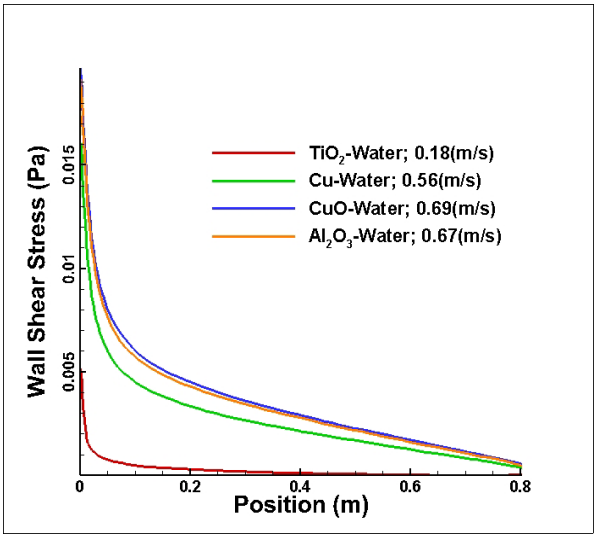

Fig. 17. Distributions of the Wall Shear Stress along the longitudinal direction, obtained by numerical method curved-wall diffusers with the nanofluids.

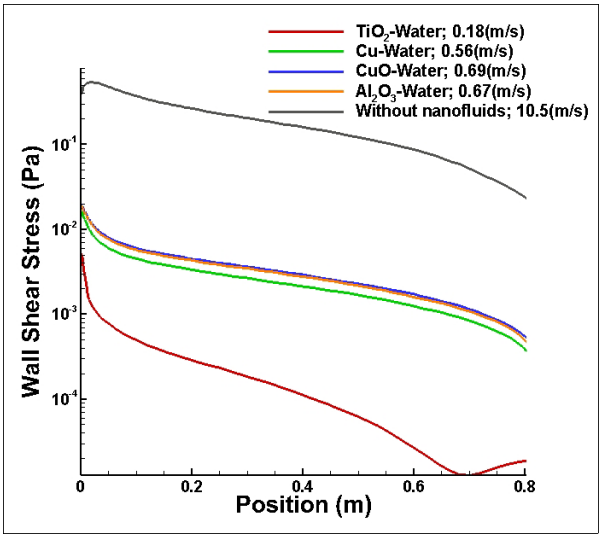

Fig. 18. Distributions of the Wall Shear Stress along the longitudinal direction, obtained by numerical method curved-wall diffusers with the nanofluids (in logarithmic scale).

In these cases, it was found that, in the whole numerical example, the results of the calculation revealed diminutive initial velocity U_0 and no significant effect on the displacement of the separation point. Also, by choosing U_0=10.5 *m/s*, the Reynolds number, R_e, did not have any significant effect on the separation point in this method of calculation. For the verification of these results, an experimental study was required to be carried out. The above calculations were studied in a numerical code, too. Numerical results were obtained using Ansys Fluent 17.2. Grid type of Quadrilaterals was selected. Several different grid distributions were examined to ensure that the calculated results are grid-independent. It can be said that by choosing 30, 60, and 300 nodes, respectively, in the inlet, outlet, and axial direction, numerical results become independent from the grid. The results have been shown in Figures 11 to 14 for the straight-wall conical diffuser and the curved-wall conical diffuser in Figures 15 to 18 with and without nanofluid. In the above-mentioned method, considering changes of the Wall Shear Stress in the longitudinal direction, tending to zero, it represents the separation point. As shown in the Figures, the presence of nanofluid is not in favor of the displacement of the separation point. Therefore, it might not be considered as a good technique for controlling separation point in diffuser's performance.

11. Conclusion

In this paper, analytical, experimental and numerical method has been analysed concerning the turbulent boundary layer in diffusers. An approximate method based on the analogy with the rheological power law in the case of Prandtl model of turbulence was investigated by two empirical constants n=0.66 and k_n=0.55. The global turbulent boundary layer in the case of axisymmetrical straight-wall conical diffusers was computed and validated with the experimental data in the literature. In Table 1, and Figures 2 to 5, it can be seen that the results are physically acceptable. In addition, it was observed that the separation point ($C_f \cong 0$) appeared with x=0.1 *m* having a relatively good agreement with the experimental results of Singh and Azad [8] with a deviation of about 5%. The global turbulent boundary layer in a case of axisymmetrical curved-wall conical diffusers was computed. The numerical results presented in Table 2 and Figs. 7 to 10. The separation point of the turbulent boundary layer appeared at about 0.55*m*, while the other global characteristics of the turbulent boundary layer can be physically acceptable. With the suitable prescribed geometrical curved-wall, the displacement of separation point was found to be significant and could be helpful in the diffuser's performance. Based on the numerical results presented in Table 3, it was found that the presence of nanofluid did not have any significant effect on the separation point. In addition, results obtained via Ansys Fluent 17.2 were similar to those obtained by the approximate method, indicating that nanofluid revealed some feeble effects, though it was not significant. Although such results were in line with the results obtained by Dehghani [15] in the case of incompressible, laminar, and Newtonian nanofluids, experimental verification and its effects on the diffuser's performance in this particular case is felt necessary in the future investigations.

Author Contributions

The manuscript was written through the contribution of all authors. All authors discussed the results, reviewed, and approved the final version of the manuscript.

Acknowledgments

The authors wish to acknowledge the reviewers who their comments helped to improve the results of this paper.

Conflict of Interest

The authors declare no potential conflicts of interest with respect to the research, authorship and publication of this article.

Funding

The authors received no financial support for the research, authorship, and publication of this article.

Data Availability Statements

The datasets generated and/or analyzed during the current study are available from the corresponding author on reasonable request.

Nomenclature

$U_0 = u_e(x=0)$	Initial velocity	θ	Diffuser half angle
$(\bar{u},\bar{v})$	Velocity components	ρ_w	Water density
u_e	External velocity	ρ_{nf}	Nanofluid density
τ_t	Shear stress global	ρ_p	Particle density
C_p	Pressure-recover coefficient	ρ_{bf}	Based fluid density (kg/m^3)
δ	Boundary layer thickness	R_e	Inlet Reynolds number
δ_1	Displacement thickness	φ	Volume fraction of nanoparticles
δ_2	Momentum thickness	μ	Dynamic viscosity
C_f	Friction coefficient	ν	Kinematic viscosity
H	Shape factor	ν_{nf}	Nanofluid Kinematic viscosity
R_1	Diffuser inlet	μ_{bf}	Dynamic viscosity of the base fluid
R_2	Diffuser outlet radius	μ_{nf}	Dynamic viscosity of the nanofluid
$R(x)$	Diffuser radius at x direction	ρ	Density

References

[1] Von Den hoff A.E., Tetervin N., Determination of General Relation for The Behavior of Turbulent Boundary layer, *Report/Patent: NACA-TR-772*, 29, 1943, 381-405.
[2] Waitman B.A. Reneau l.R., Kline S.J., Effect of Inlet Condition on Performance of Two-Dimensional Diffuser, *ASME Journal of Basic Engineering*, D83, 1961, 349-360.
[3] MOORE C.A., KLINE, S.J., Some Effects of Vanes and of Turbulence in Two-Dimensional, Wide-Angle Subsonic Diffusers, *Report TN-4080, NACA*, 1958, 93R14383
[4] FOX R.W., KLINE, S.J., Flow Regime Data and Design Method for Curved Subsonic Diffusers, *ASME Journal of Basic Engineering*, 84, 1962.
[5] Rao D.M., Raju K.N., The use of Splitters for control flow control in wide angle conical diffusers, *Bangalor, National Aeronautical Laboratory*, TN-AE, 1964, 26-64.
[6] Furuya Y., Sato T., Kushada T., Loss of Flow in the Conical Diffusers with Suction at the Entrance, *Bulletin of JSME*, 9(33), 1966, 532-556.
[7] Senoo Y., Nishi M., Improvement of the Performance of the Conical Diffusers by Vortex Generators, *ASME*, 73, 1974, 4-10.
[8] Cochran D. L., Kline S.J., The Use of Short Flat Vanes for Producing Efficient Wide-Angle Two-Dimensional Subsonic Diffusers, *NACA-TN 4309*, 1985.
[9] He Y., Kobayashi T., Numerical Prediction Of Turbulent Flow In A Conical Diffuser Using K-⊠ Model, *Acta Mechanica Sinica*, 8(2), 1992, 117-126.
[10] Apsley D.D., Leschziner M.A., *Advanced Turbulence Modelling of Separated Flow in a Diffuser: Turbulences and Combustion*, Kluwer Academic Publishers, Netherlands, 1999.
[11] Singh R.K., Azad R.S., Turbulent flow in a conical diffuser: A review, *Experimental Thermal and Fluid Science*, 13(4), 1995, 318-337.
[12] Brunn A., Nitsche W., Separation control by Periodic excitation in a turbulent axisymmetric diffuser flow, *Journal of Turbulence*, 4(9), 2003, 1-10.
[13] Charry E.M., Elkins C.J., Eaton J.K., Pressure measurements in a three-dimensional separated diffuser, *International Journal of Heat and Fluid Flow*, 30(1), 2009, 1-20.
[14] Ohlsson J., Schlatte P., Fischer P.F., Henngson D.S., Direct numerical simulation of separated flow in three-dimensional diffuser, *Journal of Fluid Mechanics*, 650, 2010, 307-318.
[15] Dehghani M., Entropy generation analysis of nanofluid forced convection in MHD plane diffuser, *Numerical Heat Transfer*, 75(9), 2019, 647-645.
[16] Askovic R., An approximate method to calculate turbulent boundary layer on an axisymmetric body, *Transactions of the Canadian Society for Mechanical Engineering*, 18(2), 1994, 111-129.
[17] Askovic R., Practical Approximate Turbulent Boundary Layer Calculation into the Divergent Rectangular Channel, *Zeitschrift für Angewandte Mathematik und Mechanik*, 1996, 76-6, 321-335.
[18] Mahbubul I.M., *Preparation, Characterization, Properties and Application of Nanofluid*, Micro and Nano Technologies, William Andrew, 2019.

How to cite this article: Sharifi Teshnizi E., Momeni F. Analytical Solutions and Analyses of the Displacement Separating Point in Diffusers, *J. Appl. Comput. Mech.*, 8(3), 2022, 891–903. https://doi.org/10.22055/JACM.2020.32954.2112